UNIVERSITY OF OKLAHOMA

GRADUATE COLLEGE

INTEGRATING EFFECTS OF GEOMECHANICS, PHASE BEHAVIOR UNDER CONFINEMENT AND PERMEABLITY AS A FUNCTION OF PORE SIZE ON GAS AND CONDENSATE PRODUCTION FROM UNCONVENTIONAL RESOURCES

A THESIS

SUBMITTED TO THE GRADUATE FACULTY

in partial fulfillment of requirements for the

Degree of

MASTER OF SCIENCE IN NATURAL GAS ENGINEERING

AND MANAGEMENT

By

GENE MASK
Norman, Oklahoma
2016

INTEGRATING EFFECTS OF GEOMECHANICS, PHASE BEHAVIOR UNDER CONFINEMENT AND PERMEABLITY AS A FUNCTION OF PORE SIZE ON GAS AND CONDENSATE PRODUCTION FROM UNCONVENTIONAL RESOURCES

A THESIS APPROVED FOR THE
MEWBOURNE SCHOOL OF PETROLEUM AND GEOLOGICAL ENGINEERING

BY

_____
Dr. Ahmad Jamili, Chair

_____
Dr. Maysam Pournik

_____
Dr. Ahmad Sakhaee-Pour

Acknowledgements

To all of those who have supported me in this endeavor thank you! To Dr. Ahmad Jamili thank you for your support, knowledge and guidance before and during this work. Your devotion and inspiration have allowed me to obtain achievements beyond the goals I set for myself. To Dr. Maysam Pournik thank you for allowing me to see beyond myself so that I am able to make significant contributions to the world. To Dr. Ahmad Sakhaee-Pour thank you for supporting me and this work.

Dr. Wu thank you for introducing me to the frame work of computer modeling and coding. Your insight allowed me to see beyond the graphic interface. To Dr. Carl Sondergeld thank you for sharing your time and knowledge of how geomechanics affects the world beyond our site. I would like to thank Alireze Sanaei for laying the foundation of my work, and Yixin Ma for the hard work and contribution to phase behavior modeling.

I would like to thank the faculty and staff members of the Mewbourne School of Petroleum and Geological Engineering for their support and dedication to providing the outstanding education from which all my work stems.

Table of Contents

List of Tables

List of Figures

Abstract

Modeling production in a naturally fractured shale gas condensate reservoir that has been stimulated in commercial simulators faces many challenges. Phase behavior and geomechanics cannot be easily incorporated and have varying effects on condensate and gas production. The physics behind these mechanisms must be carefully considered when creating the reservoir model. Phase behavior changes due to confined pore space can have a significant effect on the production which can be seen due to condensate drop out in the larger pore spaces and fractures. Geomechanics play an important role in accurately estimating the production of the reservoir as well. The effect of geomechanics on the deformation of the reservoir rock can be seen by suppressing the dew point pressure and allowing more condensates to be produced during the life of the well. Incorporating closure of the natural fractures results in a decrease in condensate production.

To better understand these mechanisms, a model of a gas condensate shale reservoir incorporating the changes in transport properties and phase behavior within nanoscale confinement was developed in compositional modeling software. A geomechanical model was iteratively coupled with the reservoir fluid flow model to investigate the impact on condensate production. Understanding the mechanisms behind condensate production will improve optimization reservoir development.

The reservoir model was created using coarse, logarithmically spaced, locally refined, dual permeability (LS-LR-DK) within the stimulated reservoir volume (SRV) and unrefined dual permeability model in the unstimulated reservoir volume (USRV). The

model represents a 1-stage hydraulically fractured well with 80 ft. cluster spacing. The reservoir and dew point pressures are 5,000 and 3,800 psia respectively. The reservoir fluid composition consists of 80% light (C_1-C_3), 10% intermediate (C_4-C_6) and 10% heavy (C_{7+}) components. The reservoir temperature is 180°F. The matrix and natural fracture permeability were 149 nD and 1 µD respectively. The effect of confinement on phase behavior is considered by changing the critical properties (T_c and P_c) of pure components according to the correlations developed by Yixin et al. (2014).

The geomechanical model incorporated the model developed by Tran et al. (2002) in order to account for porosity changes as a function of pressure, temperature and total mean stress. Matrix permeability of the USRV and SRV were modified as a function of change in mean effective stress. The natural fracture permeability changes were calculated as a function of pore pressure change. Initial values for Poisson's ratio and Young Modulus were 0.25 and $2.6e^6$ psi respectively. A value of 0.75 was used for Biot's coefficient.

The condensate production was analyzed over a 15 year time frame. Confined phase behavior of the fluid resulted in a 10.6% decrease in cumulative condensate production when compared to bulk phase behavior. The confined phase behavior of the fluids caused more fluids to drop out inside the hydraulic fractures impeding the amount of liquid production. Poisson's ratio increased from 0.15 to 0.35 resulted in a 1.4% decrease in cumulative condensate production. Young's modulus increased from $1.6e^6$ to $3.6e^6$ psi resulted in a 1.5% decrease in cumulative condensate

production. The less the reservoir rock would compact reduced the amount of condensate production. Matrix and natural fracture permeability decreased by 50% of their original values, as pore pressure decreased from 5000 to 2000 psi, resulted in a 1.2% production increase and 2.8% production decrease respectively in cumulative condensate production.

Not accounting for confined phase behavior and geomechanics can result in up to 12% variation in of cumulative condensate production estimations. Incorporating confined phase behavior results in liquid loading of the reservoir and impedes condensate production. Geomechanics related to rock deformation allow the system to more accurately predict production as pore pressure is maintained for a longer duration of time. The natural fractures provide conduits from the unstimulated area of the reservoir and significantly impact the estimations of hydrocarbon production. Understanding the interaction of fluids and reservoir rock during production will lead to improved reservoir development and simulation.

Chapter 1: Introduction

The proper development of unconventional shale gas resources is an important part of the oil and gas industry. Understanding the mechanisms behind production of shale gas condensate reservoirs will impact the development of the individual wells and fields. Research has shown that matrix, fracture permeability, fracture characteristics, PVT properties and the relative permeability are critical parameters for predicting unconventional reservoir performance (Orangi et al., 2011). By examining simulation results, engineers can better understand the critical role of how the "fracture-matrix" linear flow impacts production and that a SRV does exist around the hydraulic fractures (Wang, et. al., 2014). It also affects the economic analysis of the reserves held by the producer. By creating better models, petroleum engineers can design more efficient drilling, completion and production plans for the reservoir. Overall this leads to money saved during each of these processes. This will allow them to properly report to their employers, investors and the government the economic impact of development and production from the unconventional shale gas resources.

Commercial simulation software is limited in its ability to mimic the unconventional gas condensate reservoir. Since current equations cannot precisely predict the physics encountered, complex coding is incorporated to allow the program to produce results similar to those encountered during hydrocarbon production from unconventional shale gas condensate reservoirs.

The fluid and rock interactions in these resources make it difficult to predict the behavior of the hydrocarbon fluids as they are produced. Research has shown that

incorporating geomechanics with the reservoir fluid flow model more accurately predicts the change occurring as the reservoir is produced. As stated by Tran et al. (2009) the fundamental of geomechanics are based on Terzaghi's theory of effective stress and Biot's generalized 3D theory of consolidation and reservoir flow is based on Darcy's fluid-flow law and the conservation of mass and energy. Since these physical phenomena do interact and influence each other in a porous medium, the effective coupling between geomechanics and reservoir flow is necessary for a deformable porous medium in which pressure, temperature, fluid flow, deformation and stress must be integrated (Tran et al., 2009). As the hydrocarbons are produced, the pore pressure will decrease; thus the effective stress on the reservoir rock will increase leading to a reduction of pore and pore-throat size. A coupled flow-geomechanics model including pore confinement effects should be used to examine the behavior of unconventional shale resources (Xi et al., 2014). A decrease in the PVT phase envelopes of hydrocarbons confined in nanopores can lead to a delay in the onset of the dew point pressure and condensate liquid drop out (Altman et al., 2014). A severe drop in productivity can be observed due to matrix and fracture compaction and condensate banking (Orangi et al., 2011). In order to optimize production, iteratively coupled reservoir modeling is incorporated to create a better understanding of gas and condensate production.

This work will examine the impact of phase behavior change due to pore space confinement and geomechanics on an unconventional shale gas condensate reservoir with Eagle Ford properties. By creating a model of a single stage hydraulically fractured well, sensitivity of production dependent on for mentioned parameters will

show the predicted changes that can occur during recovery of the hydrocarbons. The results and conclusions will help engineers to understand and better predict the behavior of hydrocarbons produced in an unconventional shale gas condensate reservoir.

Chapter 2: Geomechanical Modeling

The values of Poisson's ratio and Young's modulus are important to consider when simulating hydrocarbon production. As hydrocarbons are produced, the elastic properties of the rock and in-situ stress regime change. The change in stress leads to complex is behavior of the hydrocarbons in place as they are produced. Changes in porosity, permeability and mean effective stress affect the pressure and flow of the reservoir hence the production of the hydrocarbons. Studies show that production performance is sensitive to fracture permeability and matrix relative permeability (Orangi et al., 2011). The mechanical properties obtained may be slightly to considerably different than existing in-situ conditions because reservoir rocks are often layered, fractured, faulted and jointed (Tiab and Donaldson, 2004). These properties can be quantified through downhole measurements or laboratory experimentation. The overall rock mass may be more influenced by the reactions to applied loads than by the microscopic properties of the rock matrix (Tiab and Donaldson, 2004). The geomechanical grid system allows for the simulation to account for the complex behavior of the reservoir rock during production. The importance of geomechanical effects on production modeling can be seen through this research.

The compositional simulator uses 3D finite elements that have 8 nodes locally ordered as shown below in Figure 1. The geomechanical grid is independent of the reservoir

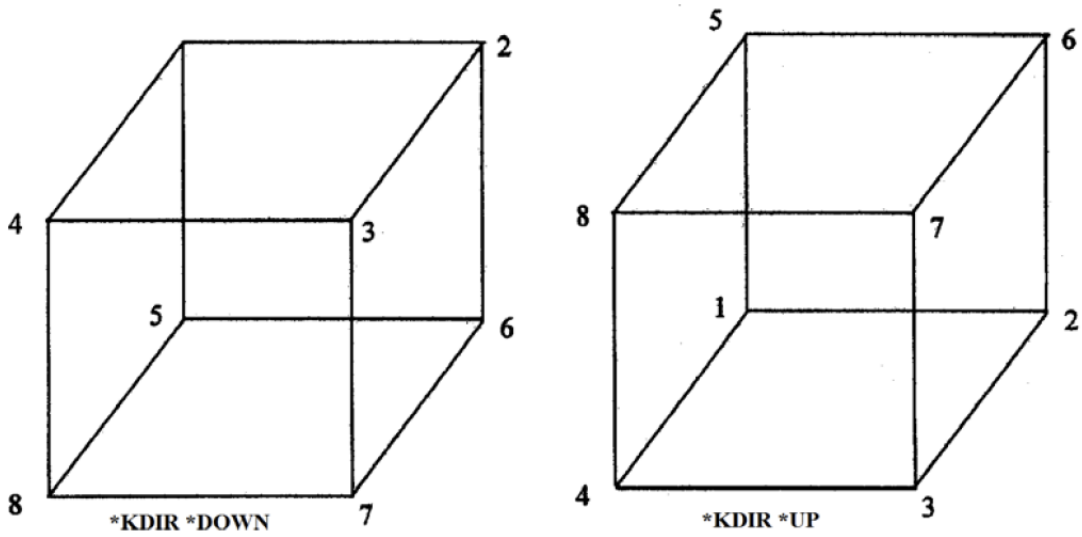

Figure 1. 8 nodes locally ordered for 3D finite elements (GEM, CMG, 2013).

fluid flow model grid with the same grid orientation in the X, Y and Z directions and contain the same common space. The model is based on plastic deformation which performs a finite-element stress analysis of the reservoir formation using a specific set of displacement and traction boundary conditions (GEM, CMG, 2013). The elastic behavior of the model is exhibited through the constant values for Young's Modulus and Poison's ratio. The plastic strain is considered irreversible after the rock reaches a yield state at a given stress level as defined by the yield criteria, Mohr-Coulomb, which is suitable for geological material (GEM, CMG, 2013). The initial stress distribution on the geomechanical grid block model can be seen in Figure 2. The normal stress on a surface perpendicular to the X axis is represented by sigma_x. The shear stress on the surface perpendicular to the X axis and its adhesive friction

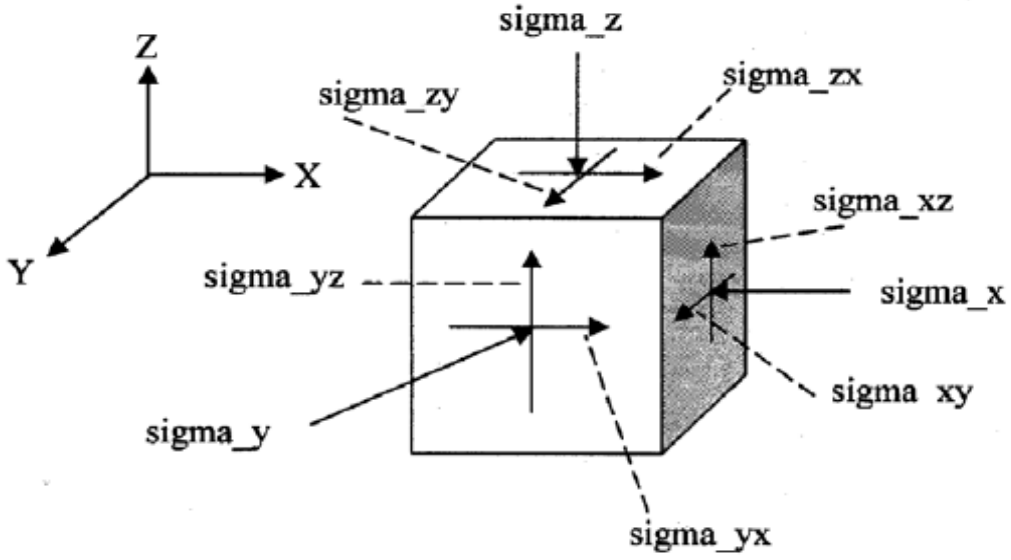

Figure 2. Stress convention used on a block in the geomechanical model (GEM, CMG, 2013).

direction is parallel to the Y axis is represented by sigma_xy (GEM, CMG, 2013). The Tran et al. model (2002) is used to incorporate porosity as a function of pressure, temperature and total mean stress in the geomechanical model. The model was developed for iterative coupling and improved accuracy in convergence coupling. The formula was developed on the basis of existing theories of Betti's reciprocal theorem and Biot's poroelasticity theory which has led to a significant reduction of the number of coupling iterations needed for converging solutions (Tran et al., 2002). The formula (2.1) based on fundamental of continuum mechanics within one time step of computation by Tran et al (2009) is as follows:

$$\phi^*_{(k+1)} = \phi^*_n + C^o_n\left(p_{(k)} - p_n\right) + C^1_n\left(T_{(k)} - T_n\right) \qquad (2.1)$$

where:

$$C_n^o = (c_0 + c_2 a_1)_n \tag{2.2}$$

$$C_n^1 = (c_1 + c_2 a_2)_n \tag{2.2}$$

$$c_0 = \frac{1}{V_b^0}\left(\frac{dV_p}{dp} + V_b \alpha c_b \frac{d\sigma_m}{dp} + V_p \beta_p \frac{dT}{dp}\right) \tag{2.3}$$

$$c_2 = -\frac{V_b}{V_b^0}\alpha c_b \tag{2.4}$$

$$a_1 = \Gamma\left\{\frac{2}{9}\frac{E}{(1-\upsilon)}(c_b - c_r)\right\} \tag{2.5}$$

$$a_2 = \Gamma\left\{\frac{2}{9}\frac{E}{(1-\upsilon)}\beta_p\right\} \tag{2.6}$$

$p_{(k)}$: pressure at kth Newton's iteration

p_n : pressure at previous time step n

$T_{(k)}$: temperature at kth Newton's iteration

T_n : temperature at previous time step n

ϕ_n* : reservoir porosity at previous time step n

ϕ_k* : reservoir porosity at kth Newton's iteration

Γ : factor that depends on the prescribed boundary conditions

σ_m : mean total stress (kPa | psi)

β_p : volumetric thermal expansion coefficient

c_b : bulk compressibility (1/kPa │1/psi)

E : Young's Modulus (kPa │ psi) * GCFACTOR

V_b : bulk volume (m^3 │ ft^3)

α : Biot number

ν : Poisson's ratio

The model allows for deformation changes in porosity to be passed to the reservoir model for fluid flow equations. Young's modulus (E) is multiplied by the GCFACTOR of (1-ν)/(1-2ν) where ν represents Poison's ratio of the porous rock and the reservoir is constrained as seen in Figure 3 below.

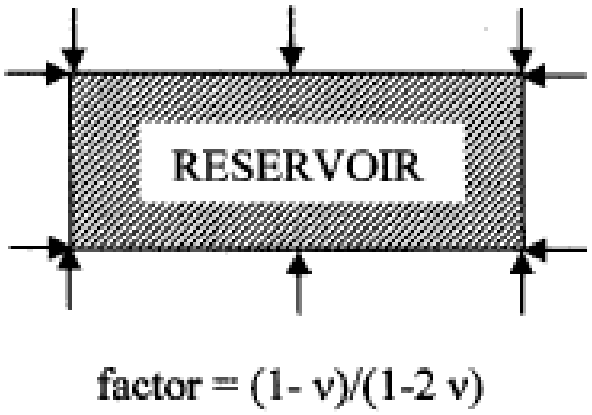

Figure 3. 2D illustration of boundary constraints on the reservoir (GEM, CMG, 2013).

Chapter 3: Reservoir Fluid Flow Modeling

The reservoir fluid flow model is based on the design by Rubin (2010) seen in Figure 4 below. Using coarse, logarithmically spaced, locally refined, dual permeability (LS-LR-DK) model to properly model naturally fractured shale with nano dary permeability. Rubin (2010) showed that the model could overcome the limitations of the MINC grid and accurately model flow in a fractured shale gas reservoir. The dual permeability model allows for simultaneous matrix-matrix and fracture-fracture flow. The local grid refinement is used to create the SRV. The logarithmically spaced grids presented by Rubin (2010) best represent the large pressure drop near the matrix-fracture (hydraulic) interface.

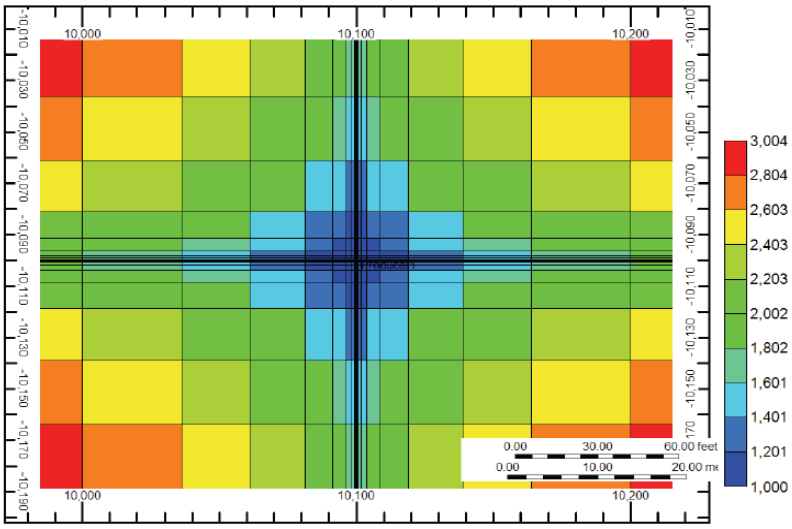

Figure 4. Single fracture network LS-LR-DK grid model proposed by Rubin (2010).

Fluid flow in a porous media is captured through Darcy's law, conservation of mass and equations of state. As stated by Tran et al. (2009) basic flow equations for a single-component single phase are as shown:

3.1 *Mass flow equation: combination of Darcy's law of fluid flow in a porous medium and mass conservation*

$$\frac{\partial}{\partial t}\left(\phi^{*}\rho_{f}\right) - \nabla\left(\rho_{f}\frac{k}{\mu}\left[\nabla p - \rho_{f} b\right]\right) = Q_{f} \tag{3.1}$$

where,

$$\phi^{*} = reservoir\ porosity = \frac{current\ pore\ volume}{initial\ bulk\ volume} = \frac{V_{p}}{V_{b}^{0}}$$

The influence of the pore walls on the fluid molecules is magnified as the pore space becomes extremely small on the nano scale. Rahmani Didar and Akkutlu (2013) explained that as pore space decreases the phase envelope of the reservoir hydrocarbons are suppressed due to the decrease in critical temperature and pressure. The suppression of the phase envelope can be seen below in Figure 5 as presented by Rahmani Didar and Akkutlu (2013). The behavior of the fluids in the matrix rock is altered to mimic this effect by including altered critical temperatures and pressures within the reservoir simulator. These altered properties coincide with the matrix rock which contains the nano sized pores.

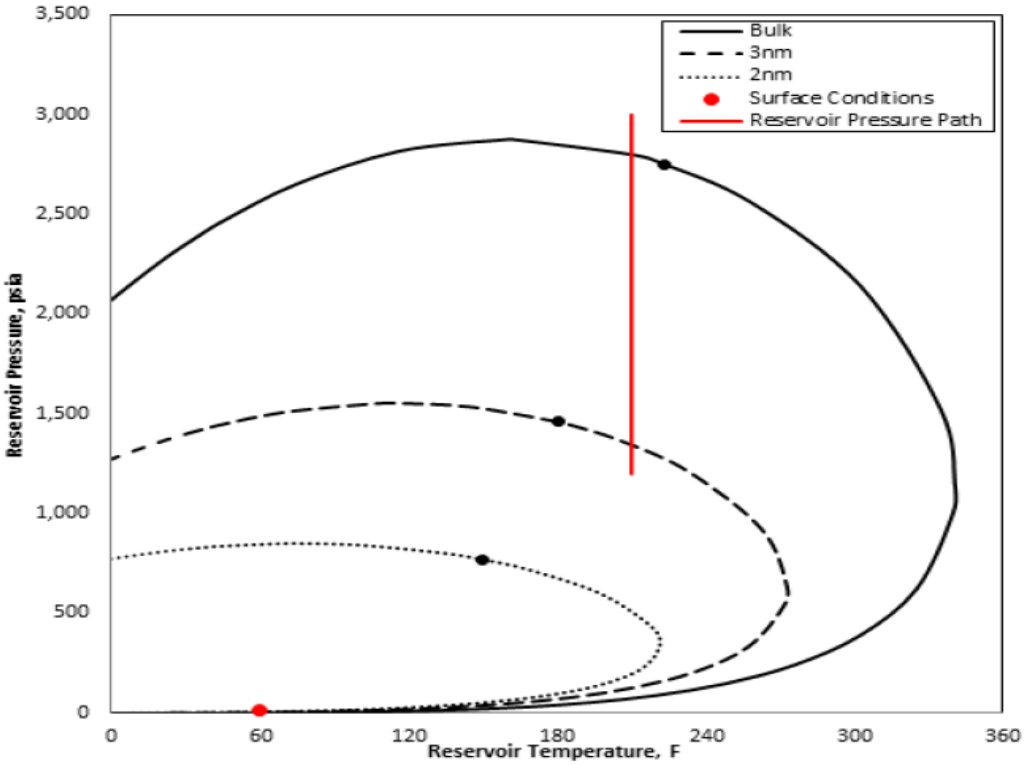

Figure 5. Depiction of the phase envelope being suppressed with decreasing pore size as shown by Rahmani Didar and Akkutlu (2013).

The reservoir model uses the modified Peng-Robinson equation of state for the fluid properties of gas and oil phases. To account for phase change behavior due to confined pore space as seen in Figure 6, the equation of state component properties for critical temperate and pressure where modified using correlations proposed by Ma et al. (2013). The changes in critical properties determined for varying levels of confinement are shown below in correlations developed by Ma et al. (2013):

$$\Delta T_c = \frac{T_c - T_{cz}}{T_c} = 1.1775 \left(\frac{D}{\sigma}\right)^{-1.338} for \left(\frac{D}{\sigma}\right) \geq 1.5 \quad (3.2)$$

$$\Delta T_c = \frac{T_c - T_{cz}}{T_c} = 0.6 \, for \left(\frac{D}{\sigma}\right) \leq 1.5 \quad (3.3)$$

$$\Delta P_c = \frac{P_c - P_{cz}}{P_c} = 1.5686 \left(\frac{D}{\sigma}\right)^{-0.783} \qquad (3.4)$$

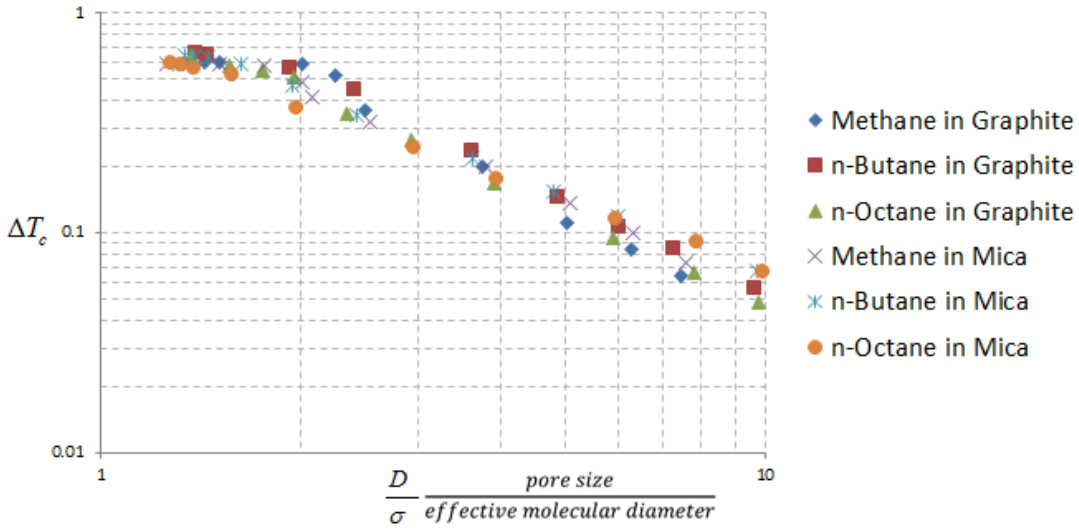

Figure 6. Critical temperature shift as a function of ratio of pore size to effective molecular diameter (Ma et al., 2013) data points from (Singh et al., 2009; Vishnyakov et al., 2001; Singh et al., 2011).

Sanaei (2014) used these correlations to integrate critical properties change under confinement into fluid-flow reservoir modeling. The model applied these component properties based on the given pore size in the reservoir model. Through this research we will developed a better understanding of how the fluid flows from the matrix rock to the larger pore spaces of the natural and hydraulic fractures can affect production in an unconventional shale gas condensate reservoir.

Chapter 4: Iteratively Coupled Reservoir Simulation

The simulation is performed by iteratively coupling between two independent grid systems of the reservoir and geomechanical models. This allows the simulator to account for the complexity of the hydraulic fracture system while performing the geomechanical calculations for the rock independent of each other. It relays the data between both grid systems over multiple iterations as seen below in the flow chart in Figure 7.

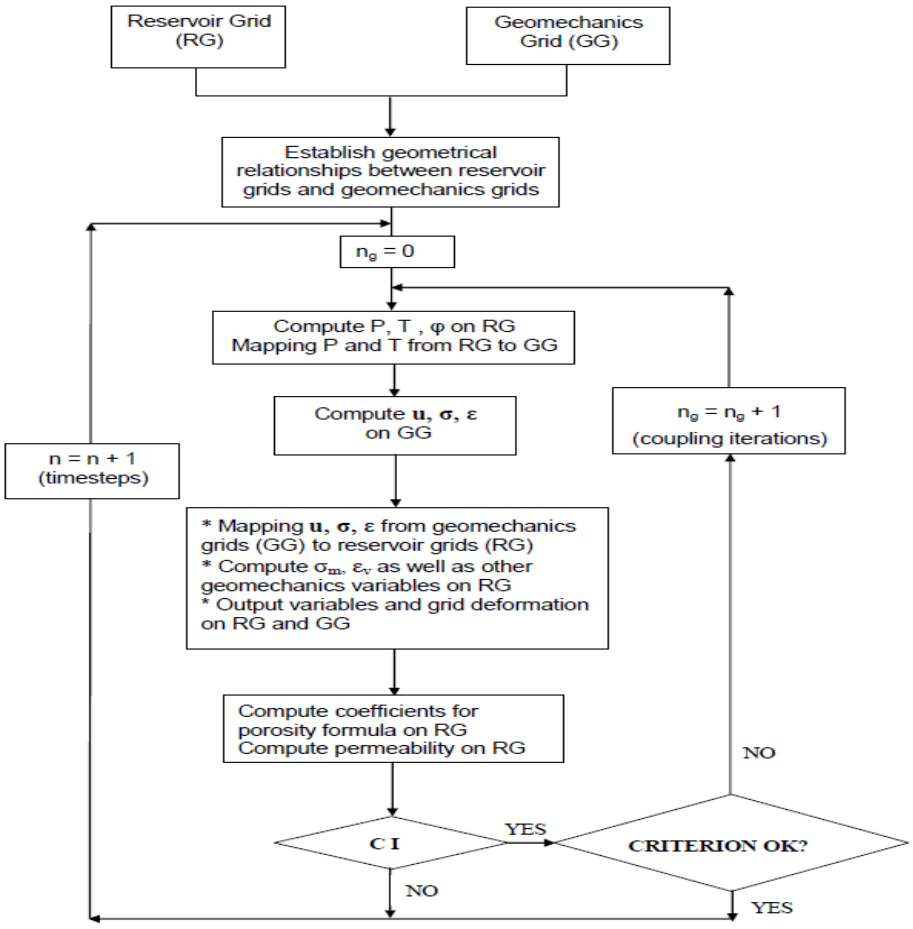

Figure 7. Flow chart for iterative time-based coupling (Tran et al., 2009)

The iterative coupling allows for the information to be passed back and forth explicitly while decreasing the run time of the simulation (Tran et al, 2005). Iterative coupling also allows the geomechanical module to be coupled with any reservoir simulator without substantial code modifications (Tran et al, 2005). While this is simply stated the process is very complicated. As explained by Tran et al. (2008), mapping must be performed for the finite difference grid of the flow variables which are calculated at the center of the blocks and finite element of the geomechanical grid model where the displacement is computed at the corners and stresses are computed at Gaussian points.

As the reservoir model becomes more complex, the run time of the simulation increases exponentially. The reservoir model has an USRV (unstimulated reservoir volume). The USRV is outside they hydraulically fractured portion of the grid system, but is naturally fractured in this model. The dual permeability model allows the simulator to account for matrix and natural fracture permeability of the reservoir. The SRV (stimulated reservoir model) accounts for the hydraulically fractured portion

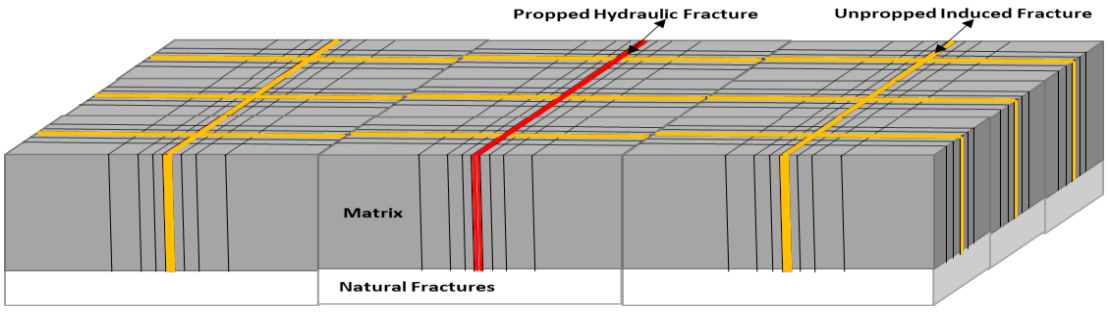

Figure 8. Depiction of SRV within a reservoir simulation (Sanaei, 2014).

of the reservoir where the horizontal wellbore is located as seen in Figure 8. It consists of hydraulic fractures, natural fractures and stimulated rock which is connected to the hydraulic fracture system via the conduits shown in the fluid-flow

reservoir grid system. Since fissures in naturally fractured reservoirs might be more stress-sensitive, the effects of geomechanics on fluid flow must be incorporated dynamically to realistically model production (Moinfar, A. et al., 2013). Recent studies have shown that unpropped natural fractures lose a significant portion of their initial permeability under pressure depletion (Cho, Y. et al., 2012). To account for the hydraulic fractures, grid cells are locally refined into smaller portions using logarithmic spacing to account for the pressure drop into the hydraulic fractures. This type of reservoir model is referred to LS-LR-DK meaning logarithmically spaced, locally refined and dual permeability as mentioned earlier. Flow conduits are also introduced into the SRV to allow for fluid flow into the hydraulic fractures.

The coupling of the fluid flow grid and geomechanical grid system allow the simulator to account for many effects often overlooked when running a singular fluid flow reservoir model. It allows for sensitivity analysis to be performed on many properties including permeability, porosity, and other stress sensitive properties of the reservoir. The effects of deformation and phase behavior can be seen in the results presented in this paper.

Chapter 5: Results

The reservoir fluid flow model incorporated a modified version of the SRV proposed by Rubin (2010). The midpoint of the conduits was altered to have matrix permeability provide a realistic flow to the hydraulically induced fractures. This system causes the fluid to flow to the hydraulic fracture that it is in the closest proximity. The fluid flow model can be seen in Figure 9 below.

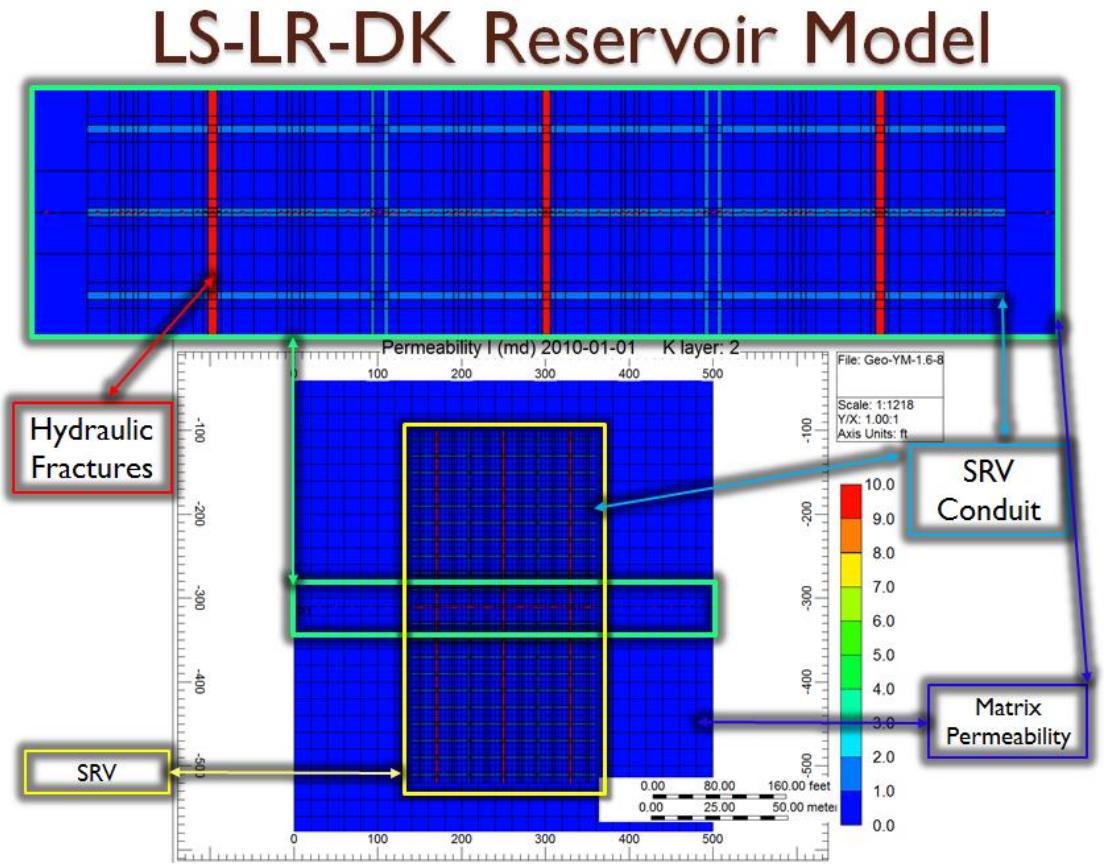

Figure 9. Reservoir fluid flow model.

The reservoir fluid composition consists of 80% light (C_1-C_3), 10% intermediate (C_4-C_6) and 10% heavy (C_{7+}) components. The reservoir and dew point pressures are 5,000 and 3,800 psia respectively. The fractions of the components are shown in

Table 1. Fractions of components for reservoir fluid flow model.

Component	Fracture %	Matrix %
N_2 to H_2S	0.796992	0.796992
IC_5 to C_{30}	7.71092	7.71092
IC_4 to NC_4	2.85897	2.85897
CH_4	71.8003	71.8003
C_3H_8	4.82295	4.82295
C_2H_6	11.3819	11.3819

Table 1. The reservoir temperature is 180°F. The single stage hydraulically fractured model with 3 clusters at 80 ft. spaces is produced for 15 years and the gas production is restricted to a maximum of 100 Mscf per day.

The geomechanical model is considered to be plastic deformation using 2.6e6 and 0.25 values for Young's Modulus and Poisson's ratio respectively based on work performed by Centurion et al. (2014), Stegen et al. (2010) and Sone and Zoback (2013) for the base case. The geomechanical grid is a Cartesian grid system similar to the fluid flow grid system, but it does not incorporate the locally refined grids of the SRV.

Table 2. Pore size and permeability by color of the reservoir model.

Permeability and Pore Size of each Region for Presented Model		
Color	Pore size	Permeability
Red	Bulk	10 mD
Light blue	Bulk	2 mD
Dark Blue	Confined ~ 15 nm	120 nD

The pore confinement effect is based on work performed by Sanaei (2014). The hydraulic fractures, natural fractures and flow conduits are represented by bulk phase behavior, and the matrix of the reservoir rock is represented by the confined phase behavior as seen in Table 2 above.

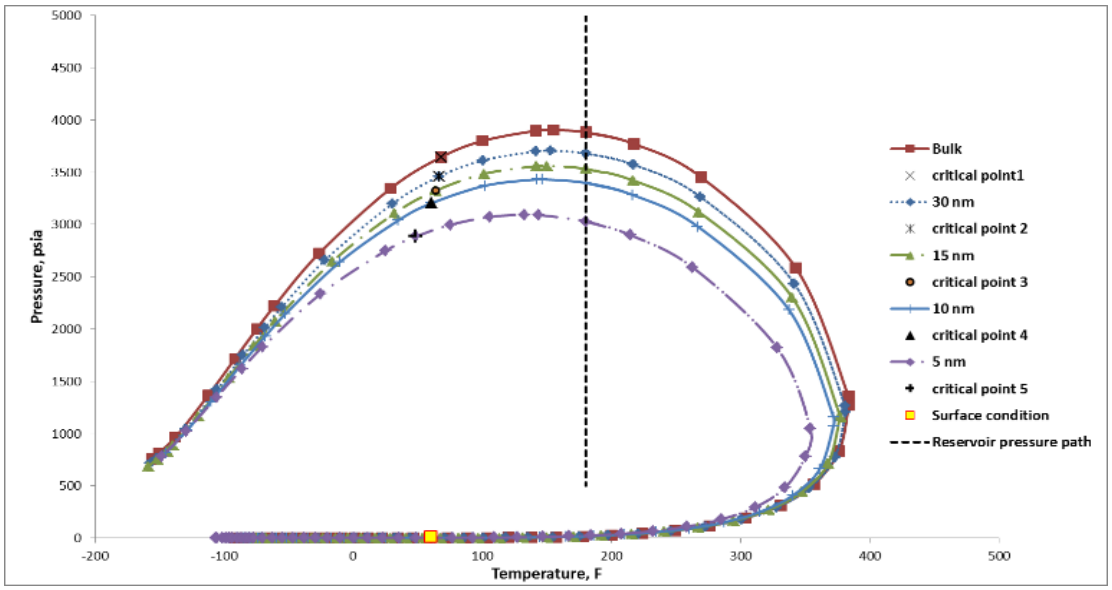

Figure 10. Effect of confinement on the two-phase envelope for reservoir gas condensate sample (Sanaei, 2014).

The confinement effect on the phase envelope can be seen above in Figure 10 based on research done by Sanaei (2014). The red phase envelope shows the unaltered phase envelope due to bulk phase behavior. The green phase envelope represents the altered phase envelope due to pore space confinement which is modeled in the simulation. As the gas flows from the smaller pore sizes of the reservoir to the larger pore space of the natural and hydraulic fractures, a significant increase in liquid saturation can be observed. The transition from gas to liquid can cause the production of the reservoir to become significantly impaired by condensate loading in the fractures.

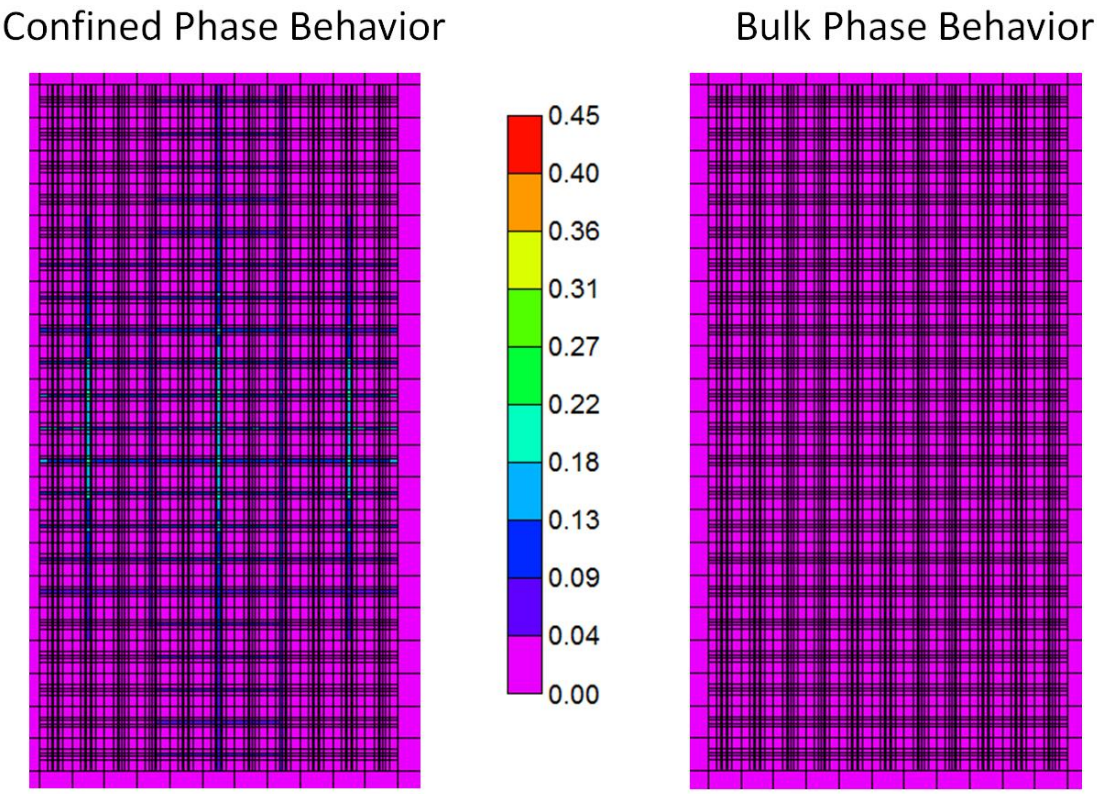

Figure 11. Shows the difference in liquid saturation after 10 months of production in the SRV.

Figure 11 shows the liquid saturation after 10 months of production in the SRV for the confined and bulk phase behavior simulations. The confined phase behavior simulation shows liquid saturation in the hydraulic fractures and conduits while the bulk phase behavior model resulted in no liquid production. As the liquid saturation profile progresses to thirteen months, the hydraulic fractures and conduits are loaded with liquids while the fluids are suppressed in the matrix. The bulk phase behavior model shows a more even distribution of fluids within the SRV at thirteen months as seen in Figure 12 below. After 15 months of production, the reservoir pressure

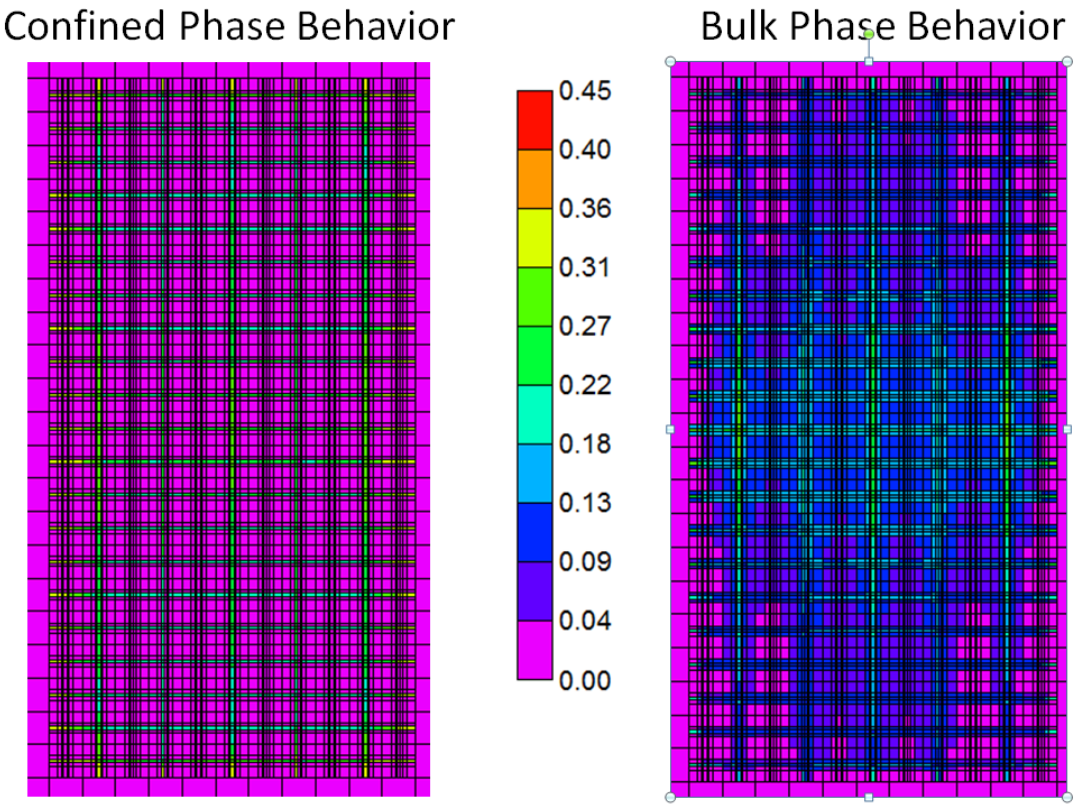

Figure 12. Shows the difference in liquid saturation after 13 months of production in the SRV.

reaches the dew point pressure of both the confined and bulk phase behavior model. This can be seen as liquids begin to form in the confined phase behavior model of Figure 13.

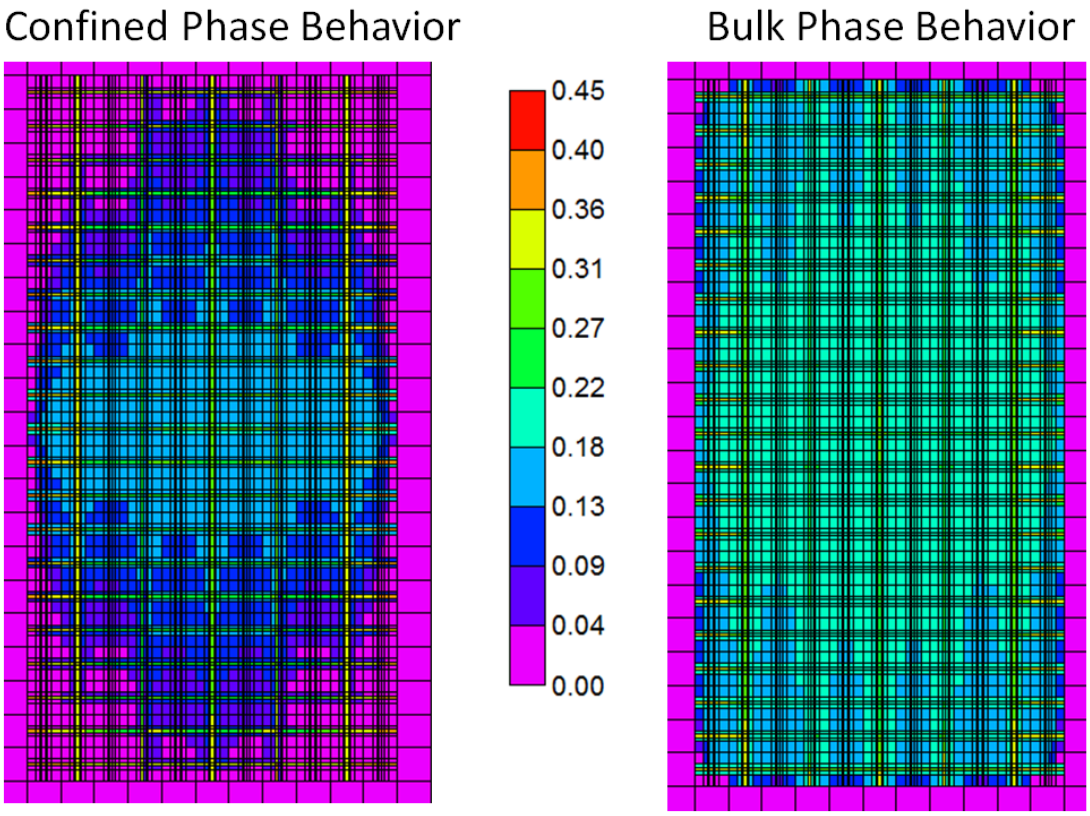

Figure 13. Shows the difference in liquid saturation after 15 months of production in the SRV.

Over time this liquid loading of the hydraulic fractures and conduits leads to decreased cumulative production of liquids from the reservoir. The confined phase behavior due to pore proximity decreased the condensate production when compared to bulk phase behavior not accounting for changes in critical temperature and pressure. Over 15 years of production, the cumulative condensate production was decreased by 10%

when accounting for the confined phase behavior due to pore proximity as seen in Figure 14 below.

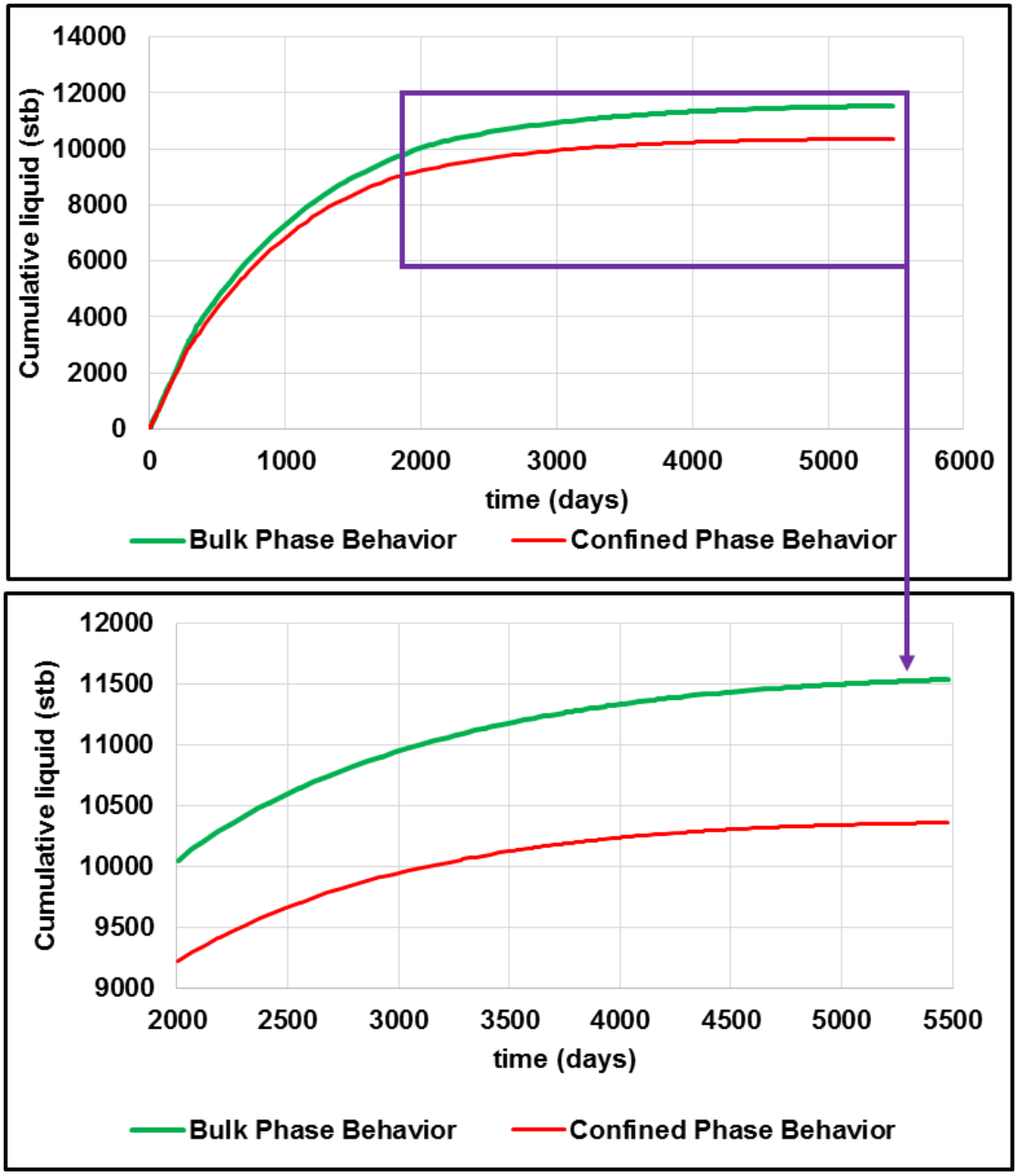

Figure 14. Cumulative liquid production versus time for bulk and confined phase behavior without geomechanics.

The confined phase behavior allows the fluids in the confined pore space to remain in the gas phase for an extended period of time due to the suppressed phase envelope. This allows the gas to be produced more quickly from the confined pore space to the unconfined space of the hydraulic and natural fractures, but liquid is formed when the gas reaches the bulk pore space where the phase envelope shifts due to lack of confinement. The liquid loading of the unconfined pore space leads to a reduction in cumulative condensate production over time. As production time increases, the impact of condensate drop out becomes apparent.

The effect of geomechanics on condensate production shows both positive and negative results. When considering the elastic properties of the reservoir, condensate production is increased over time as the rock deforms. The deformation of the reservoir rock leads to increase pore pressure over time which suppresses the dew point pressure. However, when investigating the closure of natural fractures as the pore pressure decreased condensate production decreased. The closure of the natural fractures limits the ability of the unstimulated reservoir to contribute to production. The results from the geomechanical analysis were consistent regardless of phase change behavior considerations.

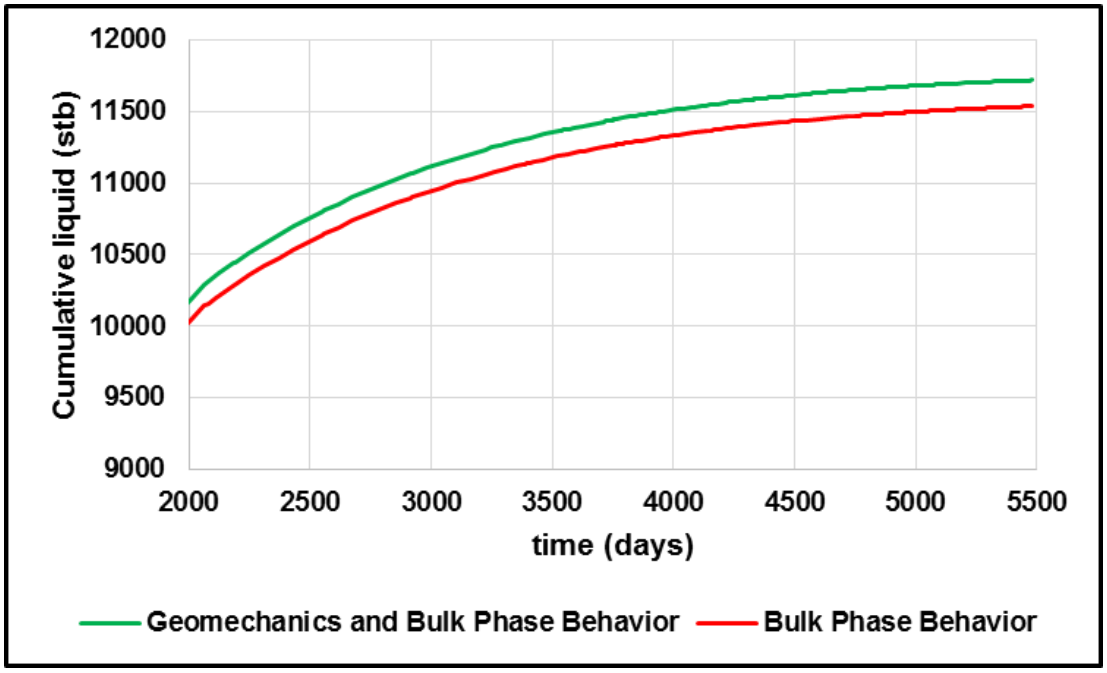

Figure 15. Cumulative liquid production versus time for bulk phase behavior with and without geomechanics.

Confined and bulk phase behavior exhibited the same trends when considering geomechanics as seen in Figures 15 and 16. The continued analysis shown of the geomechanical parameters used the concept of confined phase behavior.

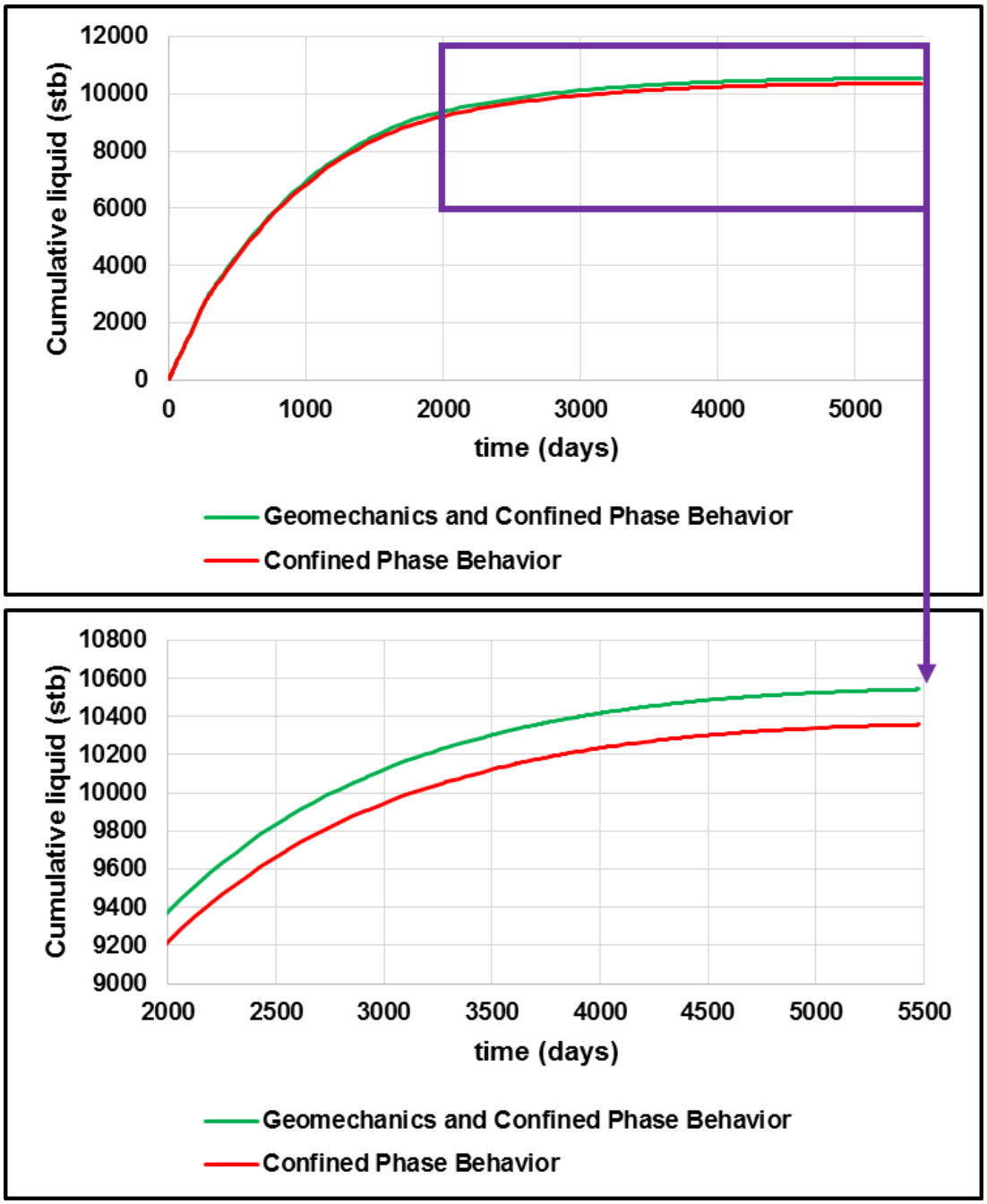

Figure 16. Cumulative liquid production versus time for confined phase behavior with and without geomechanics.

Sensitivity analysis was performed on Young's Modulus, Poisson's Ratio, matrix and natural fracture permeability. When Young's Modulus increased from 1.6e6 to 2.6e6

to 3.6e6 psi, the condensate production was reduced. The production profile for Young's Modulus as seen in Figure 17 shows a 1.5% decrease in cumulative condensate production over 15 years as Young's Modulus increased from 1.6e6 to

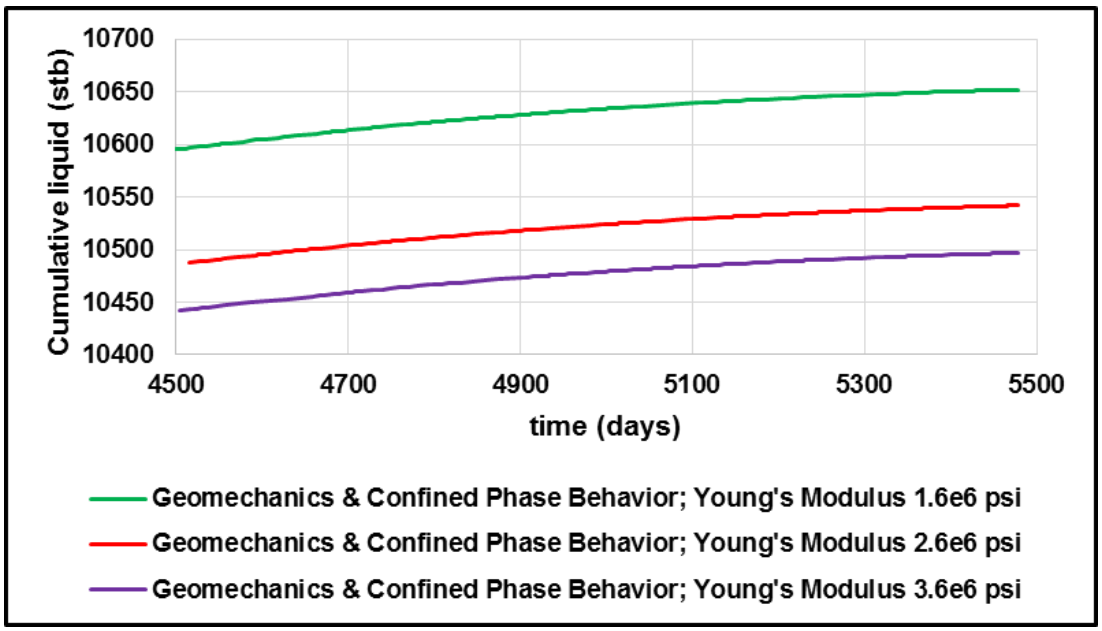

Figure 17. Cumulative liquid production versus time with geomechanics and confined phase behavior as Young's Modulus increases.

3.6e6 psi. As the rock became less ductile, the pore pressure decreased more quickly leading to the onset of the dew point pressure. The pressure profile shown in Figure 18 displays the increased pore pressure attributed to the deformation of the reservoir

rock.

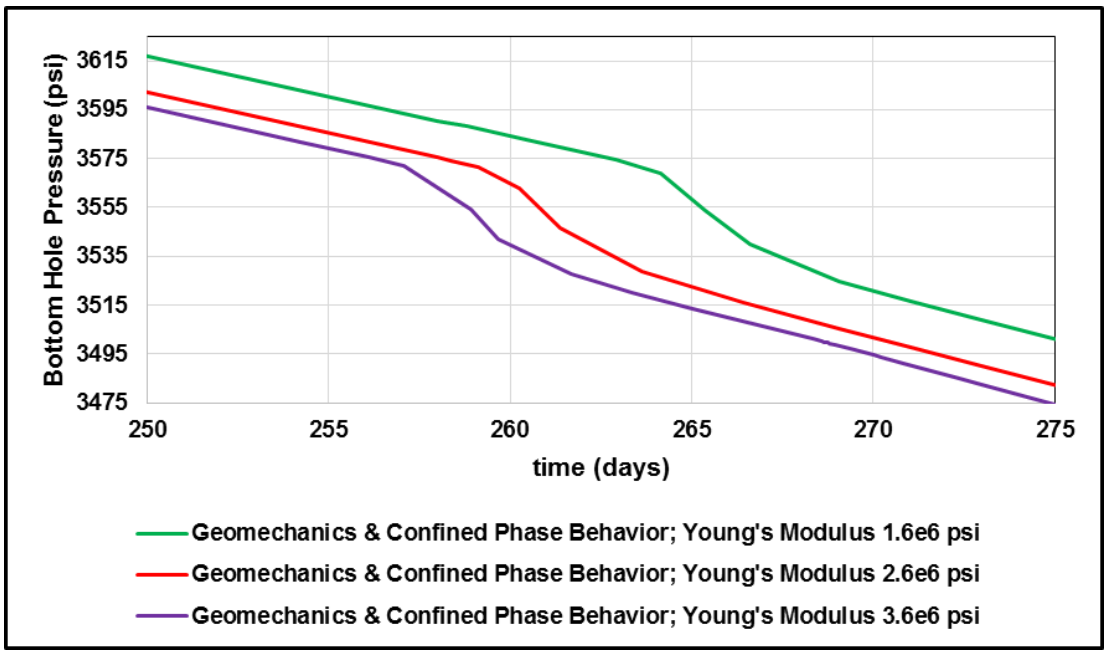

Figure 18. Bottom hole pressure versus time with geomechanics and confined phase behavior as Young's Modulus increases.

When examining Poisson's ratio, the same behavior was found in condensate production. As Poisson's ratio increased from 0.15 to 0.25 to 0.35, the cumulative condensate production decreased. The production profile for Poisson's ratio as be seen in Figure 19 shows a 1.4% decrease in cumulative condensate production over 15 years as Poisson's ratio increased from 0.15 to 0.35. The pressure profile shown in Figure 20 displays the increased pore pressure attributed to the deformation of the reservoir rock.

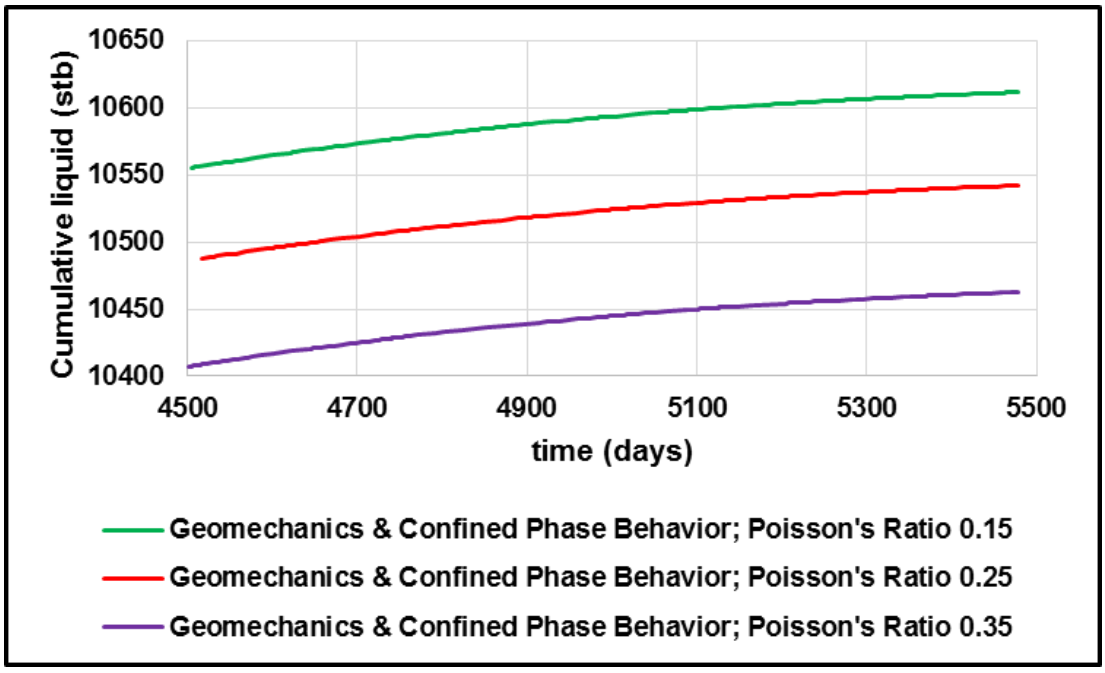

Figure 19. Cumulative liquid production versus time with geomechanics and confined phase behavior as Poisson's ratio increases.

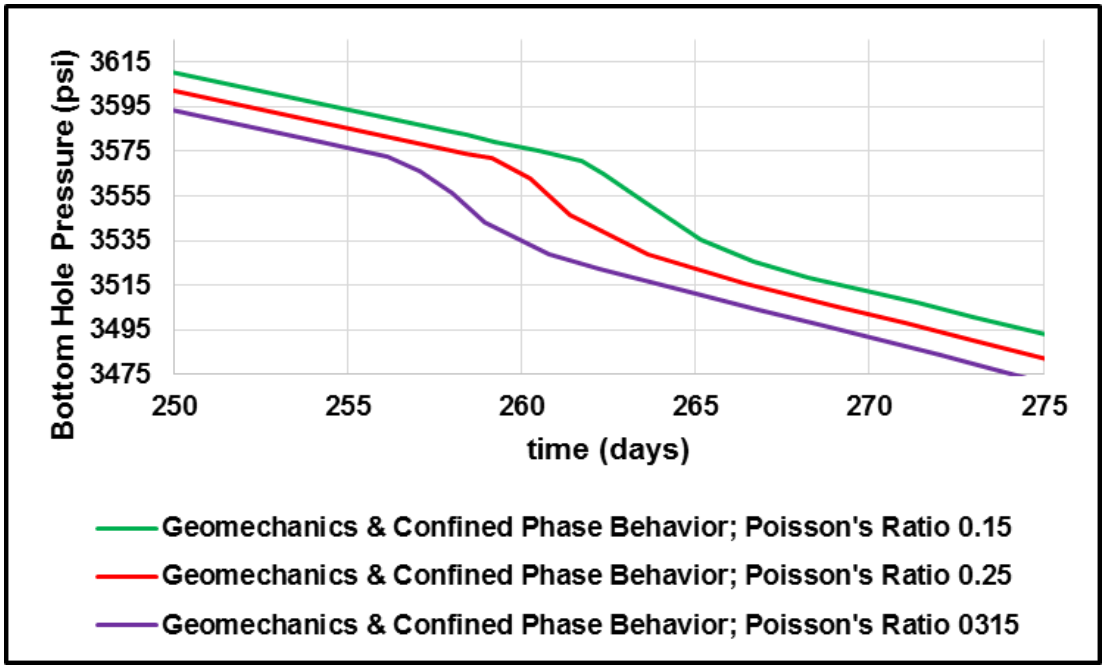

Figure 20. Bottom hole pressure versus time with geomechanics and confined phase behavior as Poisson's ratio increases.

When considering matrix permeability as a function of mean effective stress, it can be seen that as the permeability increases the condensate production increases. Figure 21 shows the cumulative condensate production increase over 15 year to be 1.2% when matrix permeability is reduced by 50% of its original value when pore pressure

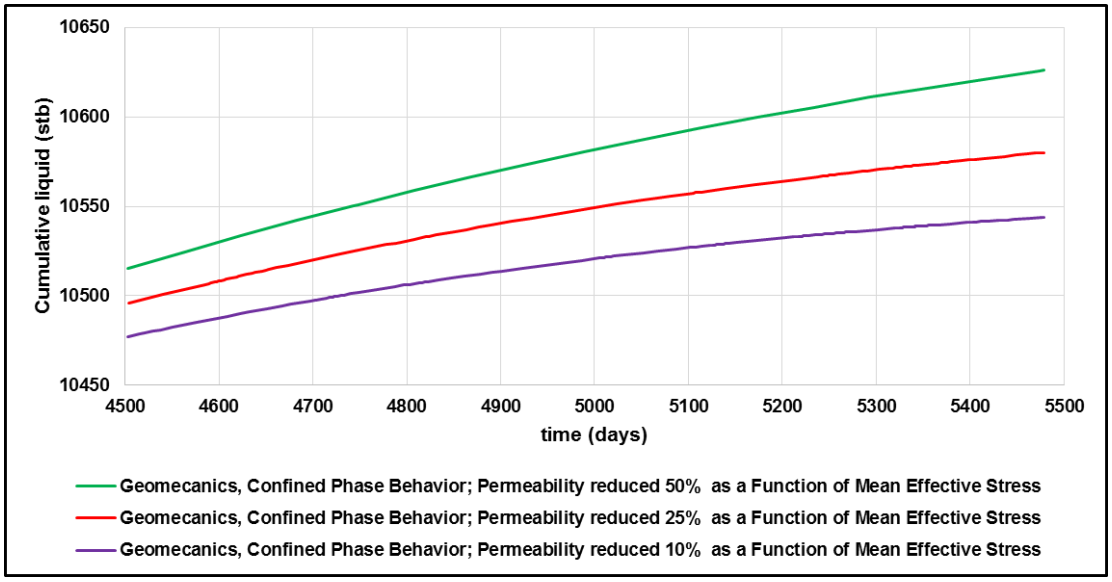

Figure 21. Cumulative production versus time with matrix permeability reduced as a function of mean effective stress.

decreased from 5000 to 2000 psi.

The sensitivity analysis of the natural fracture permeability as a function of pore pressure showed the important role natural fractures play in production. Given the earlier results, one would expect the as the natural fractures close and increase pore pressure that the condensate production would increase. Rather the opposite effect is seen during this process. As natural fractures close, cumulative condensate production is lost. Figure 22 displays that the cumulative condensate production decreased by 2.9% as natural fracture permeability is reduced by 50% of its original value when

reservoir pressure decreased from 5000 to 2000 psi. Even though pore pressure was increased as seen in Figure 23, the closure of natural fractures caused condensate

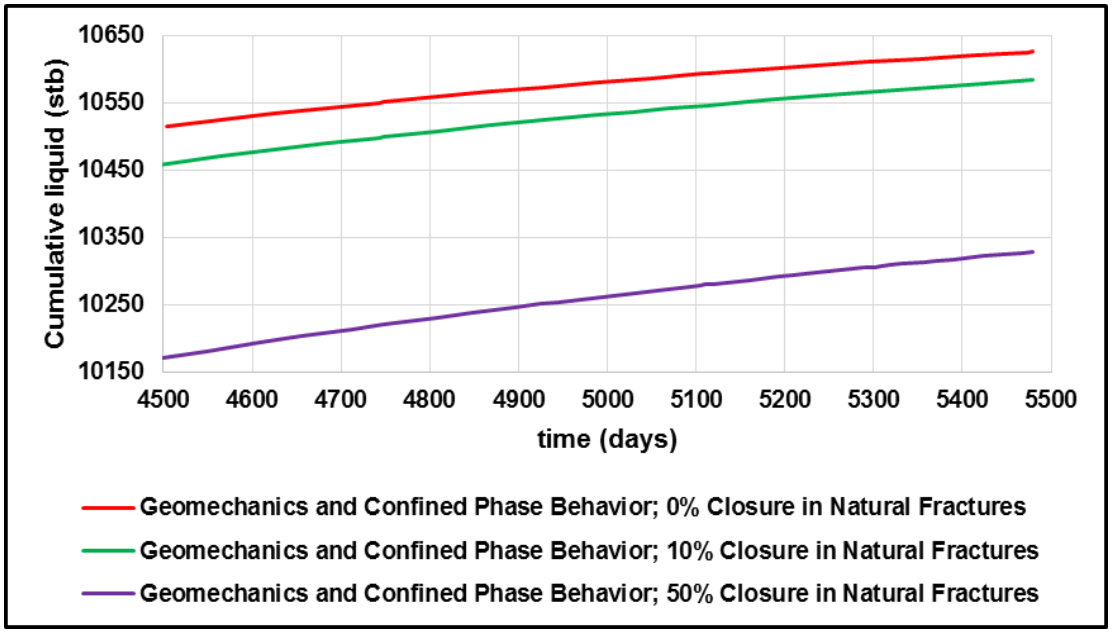

Figure 22. Cumulative production versus time as natural fracture permeability is reduced as a function of pressure.

production to be lost due to the reduced deliverability of the natural fractures. This displays the impact and importance of natural fractures on production. Without the natural fracture system to provide a conduit between the SRV and USRV production is lost even though pore pressure is increased.

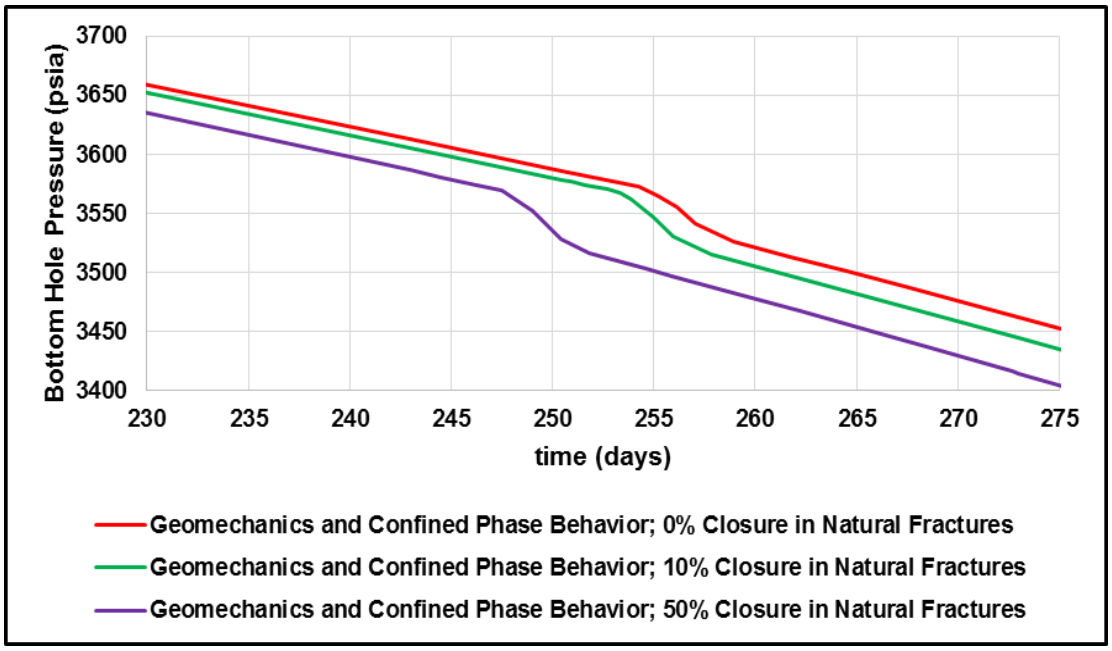

Figure 23. Bottom hole pressure versus time as natural fracture permeability is reduced as a function of pressure.

Chapter 6: Conclusions

A compositional model of a naturally fractured shale gas condensate reservoir was examined in this work. It is important to note that this represents a single stage hydraulic fractured well with 3 clusters. The amount of condensate production can increase 10 to 20 fold of the results shown on the previously shown Figures depending on the amount of stages and clusters created when fracturing a well. The independent reservoir model combined dual porosity with LS-LR-DK and was iteratively coupled with an independent geomechanical model using a compositional simulator. The effects of confined phase behavior were accounted for using modified equations of state. Changes in porosity, permeability, stress and geomchanical properties were also analyzed in the geomechanical model to show impact on hydrocarbon production. From this study we can conclude:

- Incorporating confined phase behavior due to pore wall proximity into the fluid flow model results in a decrease in cumulative condensate production over a 15 year production period. This can be attributed to condensate loading in the natural and hydraulic fractures where the pore space is considerably larger than that of the matrix.

- Incorporating geomechanics into the model to allow for compaction shows an increase in condensate production. This can be attributed to increased pore pressure which is delaying the onset of the dew point pressure.

- Closure of the natural fractures results in a decrease in condensate production due to the lost communication between the SRV and USRV.

- The SRV is primary source of condensate production during the early life of the well.
- Without incorporating dual permeability, the USRV would have minimal contribution to condensate production due to lack of natural fracture conduits connecting the SRV to the USRV.

This works shows the importance of rock and fluid properties when modeling the production of unconventional shale gas condensate reservoirs. By understanding how these properties react to the production of hydrocarbons from the reservoir, we can optimize the performance of our reservoirs.

References

Altman,R., Fan, L., Sinha, S., Stukan, M., and Viswanathan, A., 2014, "Understanding Mechanisms for Liquid Dropout from Horizontal Shale Gas Condensate Wells:, SPE 170983, presented at SPE Annual Technical Conference and Exhibition, 27-29 October, Amsterdam, The Netherlands.

Aybar, U., Eshkalak, O., Sepehrnoori, K., and Patzek, T., 2014, "Long Term Effect of Natural Fracture Closure on Gas Production from Unconventional Reservoirs", SPE 171010, presented at SPE Eastern Conference, 21-23 October, Charleston, WV, USA.

Centurion, S., Junca-Laplace, J., Cade, R., and Presley,G., 2014, "Lessons Learned From an Eagle Ford Shale Completion Evaluation", SPE 170827, presented at SPE Annual Technical Conference and Exhibition, 27-29 October, Amsterdam, The Netherlands.

Computer Modeling Group Ltd., 2013, "User's Guide GEM Compositional & Unconventional Reservoir Simulator Version 2013", 200, 1824 Crowchild Trail N.W., Calgary, Alberta Canada T2M 3Y7.

Cho,Y., Apaydin, O.G., and Ozkan, E., 2012, "Pressure-Dependent Natural-Fracture Permeability in Shale and its Effect on Shale-Gas Well Production", SPE 159801, SPE Annual Technical Conference and Exhibition, 8-10 October, San Antonio, TX, USA.

Ding, Y.D., Wu, Y., Farah, N., Cong, W., and Bourbiaux, B., 2014, "Numerical Simulations of Low Permeability Unconventional Gas Reservoirs", SPE 167711, presented at the SPE/EAGE European Conference and Exhibition, 25-27 February, Vienna, Austria

Emadi, H., Soliman, M.Y., Saumel, R., Harville, D., Gamadi, T.D., Moghaddam, R.B., 2014, "Effect of Temperature on the Compressive Strength of Eagle Ford Oil Shale Rock: An Experimental Study", IADC/SPE 167928, presented at 2014 AIDC/SPE Drilling Conference and Exhibition, 4-6 March, Fort Worth, TX, USA.

Hu, D., Matzar, L., and Martysevich, V., 2014, "Effect of Natural Fractures on Eagle Ford Shale Mechanical Properties", SPE 170651, presented at SPE Annual Technical Conference and Exhibition, 27-29 October, Amsterdam, The Netherlands.

Jin, L., Ma, Y. and Jamili, A., 2013, "Investigating the Effect of Pore Proximity on Phase Behavoir and Fluid Properties in Shale Formations", SPE 166192, presented at SPE Annual Technical Conference and Exhibition, 30 September – 2 October, New Orleans, LA, USA.

Ma, Y., Jin, L., and Jamili,A., 2013, "Modifying Van Der Waals Equation of State to Consider Influence of Confinement on Phase Behavior", SPE 166476, presented at SPE Annual Technical Conference and Exhibition, 30 September – 2 October, New Orleans, LA, USA.

Landry, C., Eichhubl, P., Prodanovic, M. and Tokan-Lawal, A., 2014, "Matrix-Fracture Connectivity in Eagle Ford Shale", URTeC 1922708, presented at Unconventional Resources Technology Conference, 25-27 August, Denver, CO, USA.

Moinfar,A., Seperhrnoori, K., Johns, R.T., and Varavei, A., 2013, "Coupled Geomechanics and Flow Simulation for an Embedded Discrete Fracture Model", SPE 163666, presented at SPE Reservoir Simulation Symposium, 18-20 February, The Woodlands, TX, USA.

Mokhtari, M., Bui, B.T., and Tutuncu, A.N., 2014, "Tensile Failure of Shales: Impacts of Layering and Natural Fractures", SPE 169520, presented at SPE Western North American and Rocky Mountain Joint Regional Meeting, 16-18 April, Denver, CO, USA.

Mokhtari, M., Honarpour, M.M., Tutuncu, A.N., and Boitnott, G.N., 2014, "Acoustical and Geomechanical Characterization of Eagle Ford Shale – Anisotropy, Heterogeneity and Measurement Scale", SPE 170707, presented at SPE Annual Technical Conference and Exhibition, 27-29 October, Amsterdam, The Netherlands.

Mullen, J., 2010, "Petrophysical Characterization of the Eagle Ford Shale in South Texas", CSUG/SPE 138145, presented at Canadian Unconventional Resources & International Petroleum Conference, 19-21 October, Calgary, Alberta, Canada.

Orangi, A., Nagarajan, N.R., Honarour, M.M., and Rosenzqeig, J., 2011, "Unconventional Shale Oil and Gas-Condensate Reservoir Production, Impact of Rock, Fluid, and Hydraulic Features", SPE 140536, presented at SPE Hydraulic Fracturing Technology Conference and Exhibition, 24-26 January, The Woodlands, TX, USA.

Rahmani Didar, B. and Akkutlu, I.Y., 2013. "Pore-Size Dependence of Fluid Phase Behavior and the Impact on Shale Gas Reservoir", SPE 168939 / URTeC 1624453, presented at Unconventional Resources Technology Conference, 12-14 August, Denver, CO, USA.

Rubin, B., 2010, "Accurate Simulation of Non-Darcy Flow in Stimulated Fractured Shale Reservoirs", SPE 132093, presented at SPE Western Regional Meeting, 27-29 May, Anaheim, CA, USA.

Sanaei, A., 2014, “Production Modeling in the Eagle Ford Gas Condensate Window”, Master’s Thesis, presented at University of Oklahoma, Norman, OK, USA.

Sanaei, A., Jamili, A., and Callard, J., 2014, “Effect of Pore Size Distrobution and Connectivity on Phase Behavior and Gas Condensate Production from Unconventional Resources”, SPE 168970, presented at SPE Unconventional Resources Conference, 1-3 April, The Woodlands, Texas, USA.

Sanaei, A., Jamili, A., 2014, “Optimum Fracture Spacing in the Eagle Ford Gas Condensate Window”, URTeC 1922964, presented at the Unconventional Resources Technology Conference, 25-27 August, 2014, Denver, CO, USA.

Sone, H. and Zoback, M.D., 2013, “Mechanical Properties of Shale-gas Reservoir Rocks – Part 1: Static and Dynamic Elastic Properties and Anisotropy”, Geophysics, Vol. 78, NO. 5, September-October.

Stegent, N.A., Wagner, A.L., Mullen, J., and Borstmayer, R.E., 2010, “Engineering a Successful Fracture-Stimulation Treatment in the Eagle Ford Shale”, SPE 136183, presented at SPE Tight Gas Completions Conference, 2-3 November, San Antonio, TX, USA.

Sutton, R.P., 1985, “Compressibility Factors for High Molecular Weight Reservoir Gases”, SPE 14265, presented at the SPE Annual Technical Meeting and Exhibition, Sept. 22-25, Las Vegas, NV, USA.

Tiab, D. and Donaldson, E.C., 2004, “Petrophysics: Theory and Practice of Measuring Reservoir Rock and Fluid Transport Properties”, 2nd Edition, Gulf Professional Publishing, Burlington, MA, USA.

Tran, D., Buchanan, L., and Nghiem, L., 2008, “Improved Gridding Technique for Coupling Geomechanics to Reservoir Flow”, SPE 115514, presented at 2008 Annual Technical Conference and Exhibition, 21-24 September, Denver, CO, USA.

Tran, D., Nghiem, L., and Buchanan, L., 2009, “Aspects of Coupling Between Petroleum Reservoir Flow and Geomechanics”, ARMA 09-89 presented at 43rd US Rock Mechanics Symposium and 4th U.S.-Canada Rock Mechanics Symposium, 28 June- 1 July, Asheville, NC, USA.

Tran, D., Nghiem, L., and Buchanan, L., 2005, “Improved Iterative Coupling of Geomechanics with Reservoir Simulation”, SPE 93244, presented at 2005 SPE Reservoir Simulation Symposium, 31 January, Houston, TX, USA.

Tran, D., Settari, A., and Nghiem, L., 2002, “New Iterative Coupling Between a Reservoir Simulator and a Geomechanics Module”, SPE/ISRM 78192, presented at SPE/ISRM Rock Mechanics Conference, 20-23 October, Irving, TX, USA.

Wang, F.P., Reed, R.M., Jackson, J.A., and Jackson, K.G., 2009, “Pore Networks and Fluid Flow in Gas Shales”, SPE 124253, presented at the SPE Annual Technical Conference and Exhibition, 4-7 October, New Orleans, LA, USA.

Xiong, Y., Winterfield, P.H., Wu, Y., and Huang, Z., 2014, ‘Coupled Geomechanics and Pore Confinement Effects for Modeling Unconventional Shale Resources”, URTeC 1923960, presented at Unconventional Resources Technology Conference, 25-27 August, Denver, CO, USA.

Yu, W., and Sepehrnoori, K., 2013, “Simulation of Gas Desorption and Geomechanics Effect for Unconventional Gas Reservoirs”, SPE 165377, presented at SPE Western Regional & AAPG Pacific Section Meeting, 19-25 April, Monterey, CA, USA.